optica

Reflection phase microscopy using spatio-temporal coherence of light

YOUNGWOON CHOI,[1,2,*] POORYA HOSSEINI,[3] JEON WOONG KANG,[3] SUNGSAM KANG,[3] TAESEOK DANIEL YANG,[1] MIN GYU HYEON,[4] BEOP-MIN KIM,[1,2,4] PETER T. C. SO,[3,5] AND ZAHID YAQOOB[3]

[1]School of Biomedical Engineering, Korea University, Seoul 02841, South Korea
[2]Department of Bio-convergence Engineering, Korea University, Seoul 02841, South Korea
[3]Laser Biomedical Research Center, Massachusetts Institute of Technology, Cambridge, Massachusetts 02139, USA
[4]Department of Biomicro System Technology, Korea University, Seoul 02841, South Korea
[5]Mechanical and Biological Engineering Departments, Massachusetts Institute of Technology, Cambridge, Massachusetts 02139, USA
*Corresponding author: youngwoon@korea.ac.kr

Published 15 November 2018

This document provides supplementary information to "Reflection phase microscopy using spatio-temporal coherence of light," https://doi.org/10.1364/OPTICA.5.001468. We discuss how the combination of temporal gating and spatial decorrelation generates a single gating which is narrower than each alone. We also describe the formation of the reflection signal from the inter-cellular membrane and its interpretation. In addition, we discuss how to eliminate the system vibrations from the cellular membrane fluctuations. Finally, we provide the MSD plots for the cellular membrane fluctuation as a supplemental analysis.

1. Theoretical model of the system

In this section, we discuss the theoretical analysis of the spatio-temporal coherence gating in our reflection phase microscope. Following the derivation of 3D transfer functions in Refs. [1, 2], the 1D transfer function can be expressed as a function of wave vector k_z, and angular frequency ω as:

$$\Gamma(k_z,\omega)=\frac{\pi}{2c^2}\omega^2 S(\omega)P(k_z,\omega)\,, \qquad \text{(S1)}$$

where c is speed of light, and $P(k_z, \omega)$ is axial aperture function defined in Eq. (2) of the main manuscript. Then the 2D Fourier transform of Eq. (S1) with respect to k_z and ω gives us the complex line-spread function of our system as:

$$\gamma(z_s,\tau_R)\propto\iint\omega^2 S(\omega)P(k_z,\omega)\exp(ik_z z_s+i\omega\tau_R)dk_z d\omega\,, \qquad \text{(S2)}$$

where z_s is the axial position of sample mirror and τ_R is the arrival time. Note that $\tau_R = 0$ results in the Eq. (1) in the main manuscript.

Now, let us consider the two experimental scenarios – without and with dynamic speckle illumination as shown in Fig. S1(a) and S1(c), respectively. Without dynamic speckle illumination, the axial aperture function becomes a delta function $P(k_z,\omega)=\delta(k_z-n_0\omega/c)$. Substituting it into Eq. (S2) yields:

$$\gamma(z_s,z_R)=\int\omega^2 S(\omega)\exp[i\omega(n_0 z_s+z_R)/c]d\omega\,, \qquad \text{(S3)}$$

where $z_R = c\tau_R$ is the optical path length delay. The above equation is identical to the Fourier transform of source spectrum $\omega^2 S(\omega)$. Therefore, by measuring the axial response of the system without the dynamic speckle illumination, we can calibrate the spectrum of the light source as shown in Fig. S1(b). The resulting multi-peak spectrum illustrates the spectral complexity of the super-continuum laser source.

Finally, we can obtain the theoretical expectation of axial response of the system with the dynamic speckle illumination by substituting the source spectrum obtained in Fig. S1(b) into Eq. (S2). As shown in Fig.S1(c)-(d), the experimental result agrees extremely well with the theoretical model for both the amplitude and the phase.

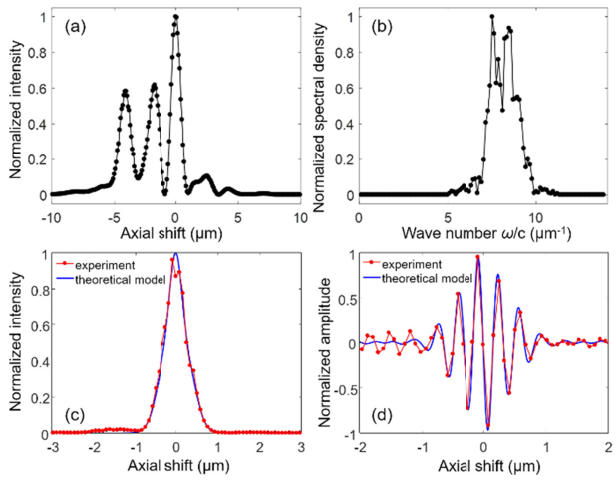

Fig. S1. (a) Axial response of the system without dynamic speckle illumination. (b) Power spectral density of the super-continuum laser, reconstructed from the measured axial response function in (a). (c)-(d) : Axial response of the system and real part amplitude, respectively, under the dynamic speckle illumination.

2. Interpretation of the reflection phase from the intercellular membrane

In a transmission measurement, the phase of light is determined by the refractive index contrast, i.e., the refractive index difference between the sample and the surrounding medium, and the thickness of the sample. In contrast, if we are interested in the outer most surface, the refractive index of the host medium and the morphological shape of the sample determine the phase in a reflection measurement [3-5]. The phase of the returning light associated with an inner surface, in general, involves both the above two mechanisms. For instance, in the case of the nuclear membrane as shown in Fig. S2, the returning light undergoes two transmission events and a single reflection event in between. The light first meets the plasma membrane and propagates through the cytosol until it reaches the nuclear membrane. After being reflected off by the nuclear membrane, it returns though the same cytosol as shown in Fig. S2. The relative phase that the reflected light obtains by the two transmissions in conjunction with the single reflection is determined as

$$\phi = 2(n_c - n_m)kL_c + 2n_c kL_n, \qquad \text{(S4)}$$

where $k=\lambda/2\pi$ with a wavelength of the light source, n_c and n_m are the refractive indices of the cytosol and the host medium, respectively, L_c is the distance between the plasma membrane and the plane of reference (PR), and L_n is the distance between the nuclear membrane and the plane PR. The first term represents the phase associated with two transmissions whereas the second term represents the reflection phase relative to the reference light. The two distances L_c and L_n fluctuate around certain mean values, l_c and l_n and thus can be represented with the mean values as $L_c=l_c+\delta l_c$ and $L_n=l_n+\delta l_n$ with the fluctuation terms δl_c and δl_n, respectively. The reflection phase then can be written as

$$\begin{aligned}\phi &= 2\Delta nk(l_c+\delta l_c) + 2n_c k(l_n+\delta l_n) \\ &= 2k(\Delta n l_c + n_c l_n) + 2\Delta nk\delta l_c + 2n_c k\delta l_n,\end{aligned} \qquad \text{(S5)}$$

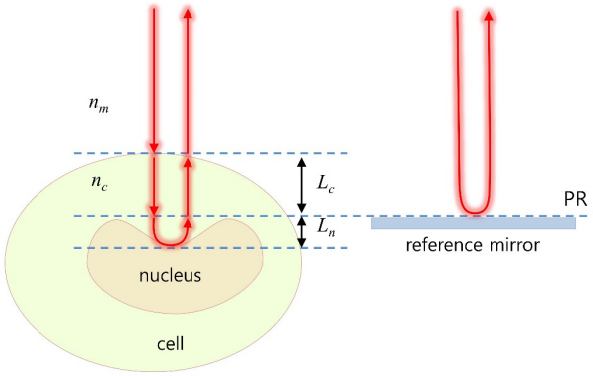

Fig. S2. Interpretation of the reflection phase. L_c: distance from the plasma membrane to PR, L_n: distance from PR to the nuclear membrane, PR: plane of reference.

where Δn is the refractive index difference. In the second expression in Eq. (S5), the first term is an overall phase, which is a constant in general and is of no interest. Thus, it can be dropped with no loss of generality. The second and the third terms are the fluctuations in transmission and the reflection phases, respectively. Since the refractive index of a cell is very close to that of the culture medium, the refractive index difference Δn is typically of the order of 10^{-2}, and is much smaller than n_c [6]. Consequently, the second term is expected to be negligible compared to the third term, unless the fluctuation of the first surface, δl_c, is sufficiently larger than that of δl_n, the fluctuation of the second surface of the cell. With this assumption, Eq. (S5) can be written approximately as

$$\phi \approx 2n_c k\delta l_n. \qquad \text{(S6)}$$

In order to assess the validity of this assumption, we performed a separate measurement of the plasma membrane fluctuations. For this purpose, we set the focus on the top plasma membrane of the cell and measured the phase of the light reflected from the surface, as done with RBCs in Ref. [5]. From the phase fluctuations associated with the plasma membrane, we obtain the corresponding height fluctuations without any ambiguity, which is typically the case with the transmission phase measurements. We quantified the RMS value of plasma membrane fluctuations as 18.1 nm [see Fig. 4 in the main text]. This value is in the same order of the nuclear membrane fluctuation described in the main text. We repeated this measurement with several cells and all measured values were in the range of 16 nm to 40 nm in RMS. This confirms that the variation in the transmission phase due to fluctuations of the plasma membrane is hundred times smaller than that of the reflection phase due to the motion of the nuclear membrane when measured in a reflection.

3. Scheme for the phase stabilization

When performing time-laps measurements in an interferometric approach, phase noise induced by the separate optical paths is always a concern. In a transmission measurement, a blank background without a sample can be used as reference to trace and remove the phase noise. However, in a reflection measurement such phase tracing is difficult due to the absence of a clean background, especially when the imaging focus lies in the middle of the sample.

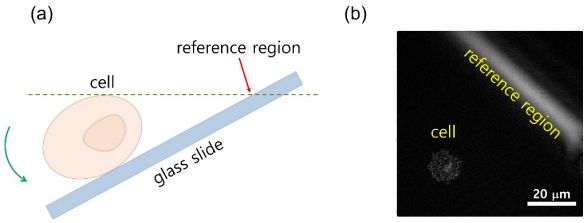

Fig. S3. Phase stabilization by tilting the glass slide. (a) Schematic for the tilt of the sample. Some blank region of the glass slide can be seen in the field of view. (b) A typical reflection image after the tilt. The clean background in the image was used to trace the phase noise in the time-laps reflection measurements.

To solve this problem, we tilted the slide glass so that a portion of the slide glass came in the field of view together with the cells [7]. The schematic is presented in Fig. S3(a). The tilting angle was about 9.2 degrees with respect to the horizontal plane. With this configuration small portion of the glass slide can be simultaneously imaged in the field-of-view as shown in Fig. S3(b). Since the phase change in the background region is only caused by the pathlength variations between sample and reference arms, we can use it as a reference region to track and remove the system phase noise. As shown in Fig. 4(e) in the main text, the phase noise measured in our system was typically tens of nanometers. This is comparable to the nuclear motions, and thus can significantly corrupt the reflection phase measurements. After removal of the phase noise, the system fluctuation reduced to 1.3 nm, which is the final sensitivity of our reflection measurements.

4. Mean square displacement of the phase fluctuations

As a metric of the quantification of fluctuation, we also calculated the mean square displacement (MSD) of the phase variation presented in Fig. 4 of the main text. The MSD is defined as [4, 8, 9]

$$\mathrm{MSD} = \left\langle \left[\phi_R(t+\tau) - \phi_R(t)\right]^2 \right\rangle_t, \qquad \text{(S7)}$$

where $\langle\ \rangle_t$ denotes the time average and τ is the time delay. The result is shown in Fig. S4. For the background fluctuation measured in the blank area, the MSD remains almost zero with no noticeable variation. In contrast, the MSD of plasma membrane gradually increased during the early time delay and later reached a plateau. On the other hand, the MSD for the nuclear membrane shows more dramatic change over time. It increased faster than that of the plasma membrane and showed a couple of humps. The rate of increase slowed over time.

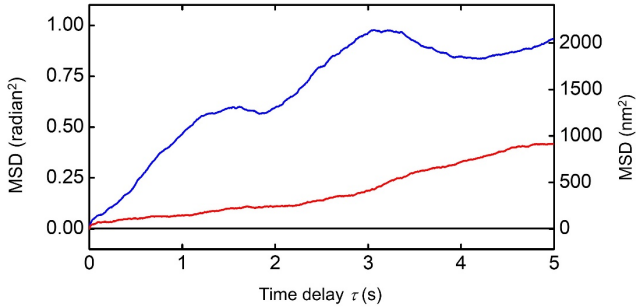

Fig. S4. MSDs for the cell presented in Fig. 4 in the main text. Blue, red and black lines represent the MSDs for the nuclear membrane, plasma membrane, and background fluctuations, respectively.

References

1. R. Zhou, T. Kim, L. L. Goddard, and G. Popescu, "Inverse scattering solutions using low-coherence light," Opt Lett **39**, 4494-4497 (2014).
2. R. Zhou, D. Jin, P. Hosseini, V. R. Singh, Y.-h. Kim, C. Kuang, R. R. Dasari, Z. Yaqoob, and P. T. C. So, "Modeling the depth-sectioning effect in reflection-mode dynamic speckle-field interferometric microscopy," Opt Express **25**, 130-143 (2017).
3. M. A. Choma, A. K. Ellerbee, C. Yang, T. L. Creazzo, and J. A. Izatt, "Spectral-domain phase microscopy," Opt Lett **30**, 1162-1164 (2005).
4. T. Yamauchi, H. Iwai, and Y. Yamashita, "Label-free imaging of intracellular motility by low-coherent quantitative phase microscopy," Opt Express **19**, 5536-5550 (2011).
5. Y. Choi, P. Hosseini, W. Choi, R. R. Dasari, P. T. C. So, and Z. Yaqoob, "Dynamic speckle illumination wide-field reflection phase microscopy," Opt Lett **39**, 6062-6065 (2014).
6. B. Rappaz, P. Marquet, E. Cuche, Y. Emery, C. Depeursinge, and P. Magistretti, "Measurement of the integral refractive index and dynamic cell morphometry of living cells with digital holographic microscopy," Opt. Express **13**, 9361-9373 (2005).
7. Z. Yaqoob, T. Yamauchi, W. Choi, D. Fu, R. R. Dasari, and M. S. Feld, "Single-shot full-field reflection phase microscopy," Opt Express **19**, 7587-7595 (2011).
8. G. Popescu, Y. Park, N. Lue, C. Best-Popescu, L. Deflores, R. R. Dasari, M. S. Feld, and K. Badizadegan, "Optical imaging of cell mass and growth dynamics," Am J Physiol-Cell Ph **295**, C538-C544 (2008).
9. N. T. Shaked, L. L. Satterwhite, N. Bursac, and A. Wax, "Whole-cell-analysis of live cardiomyocytes using wide-field interferometric phase microscopy," Biomed Opt Express **1**, 706-719 (2010).